IL NUOVO CIMENTO Vol. 34 C, N. 5 Settembre-Ottobre 2011
DOI 10.1393/ncc/i2011-10994-6

Communications: SIF Congress 2010

# Study of the bolometers thermal response for the search of rare events

V. Di Biagio(*)
*Dipartimento di Fisica, Sapienza Università di Roma - Rome, Italy*

(ricevuto il 30 Dicembre 2010; approvato il 14 Luglio 2011; pubblicato online il 5 Ottobre 2011)

**Summary.** — Large-mass bolometers are calorimeters working at low temperatures widely used in particle physics experiments to search for rare events. These devices are able to detect particles energies from few keV up to several MeV, but their response function is not linear and depends on the operating temperature. This study was performed with the bolometers of the CUORE experiment. In a previous work the non-linearities were attributed to the thermistor and to its biasing circuit and an algorithm was derived to obtain a linear response. In this work an improvement of the algorithm is proposed and the possibility of developing a more complete model of the response function, which accounts for the electrothermal feedback induced by the thermistor, is evaluated.

PACS 29.40.Vj – Calorimeters.

## 1. – Introduction

Bolometers are detectors in which the energy of the particle interactions is converted into phonons and measured via the resulting temperature variation. Owing to their excellent energy resolution, bolometers are used in particle physics experiments searching for rare events, like Neutrinoless Double-Beta Decay and Dark-Matter interactions.

The CUORE experiment (Cryogenic Underground Observatory for Rare Events) will search for Neutrinoless Double-Beta Decay in $^{130}$Te [1], using crystals of $TeO_2$ as both emitters and absorbers and NTD-Ge semiconductor thermistors [2, 3] as temperature sensors. The experiment is in progress at Laboratori Nazionali del Gran Sasso (LNGS of the INFN), in Italy, and tests are in the meanwhile conducted. Bolometers are hosted in a cryostat operating at about 10 mK and have an energy response extending from few keV up to several MeV. Over this range the energy resolution is kept almost constant at few keV, but the response function is non-linear. The conversion from signal amplitude to energy is not direct and requires the use of a calibration function. The signal amplitude

(*) E-mail: valeria.dibiagio@roma1.infn.it

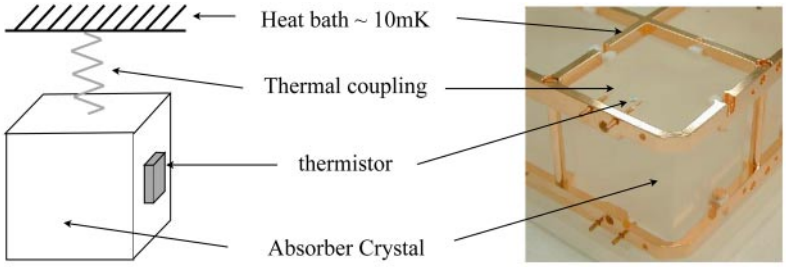


Fig. 1. – General scheme of a bolometer (left) and a CUORE bolometer (right).

depends also on the working temperature, which cannot be mantained strictly constant, so that the detector resolution can be worsened. Moreover, the shape of the signals depends on their energy, making hard the pulse shape discrimination. Understanding the sources of non-linearities is therefore necessary to improve the detector performance.

Electrothermal models of bolometers have been already proposed [4-6]. However, they rely on parameters difficult to be measured in working conditions, so they provide only qualitative descriptions of the detector features, like the signal shape. On the contrary, this article proposes a model based on few measurable parameters and usable to linearize the bolometers response function.

## 2. – Description of the detector

A CUORE bolometer is made up of two main parts, a $TeO_2$ crystal and a NTD-Ge thermistor. The cube-shaped crystal is held by teflon supports on copper frames, which are connected to the mixing chamber of a diluition refrigerator. The thermistor, that acts as a thermometer, is glued to the crystal and its biasing wires are glued to the copper frames (see fig. 1). The crystal weighs 750 g and its heat capacitance $C$ at the working temperature of 10 mK is of order 2 nJ/K [7]. When an amount of energy $E$ is released on the inside, the crystal temperature increases by $E/C$ and then returns back to the equilibrium through the thermal conductance of the supports and of the thermistor. This latter converts the temperature, $T$, into resistance, $R$, according to the relationship

$$R = R_0 \exp\left[\frac{T_0}{T}\right]^{\gamma}, \tag{1}$$

where $R_0$ and $T_0$ are parameters that depend on the dimensions and on the material of the thermistor [8]. Their value is determined experimentally and is about 1.1 Ω and 3.4 K, respectively. At 10 mK, the parameter $\gamma$ can be considered constant and equal to $\frac{1}{2}$ [9, 10], and the value of $R(T)$ is of order 100 MΩ. The bolometer temperature varies with time, hence the resistance of the thermistor is a function of the time via the temperature.

To read out the signal, the thermistor $R(t)$ is inserted in a biasing circuit, which includes in series a constant voltage generator $V_{\mathrm{B}}$ and a load resistance $R_{\mathrm{L}}$. The value of $R_{\mathrm{L}}$ is much higher than $R(t)$, so that the voltage signal $V(t)$ at the two ends of the thermistor is almost proportional to $R(t)$. The biasing wires of the thermistor have a non-negligible parasitic capacitance $c_{\mathrm{p}}$, between them and with respect to the ground, that relies on the material and on the lenght of the wires (see fig. 2(a)). Typical values of

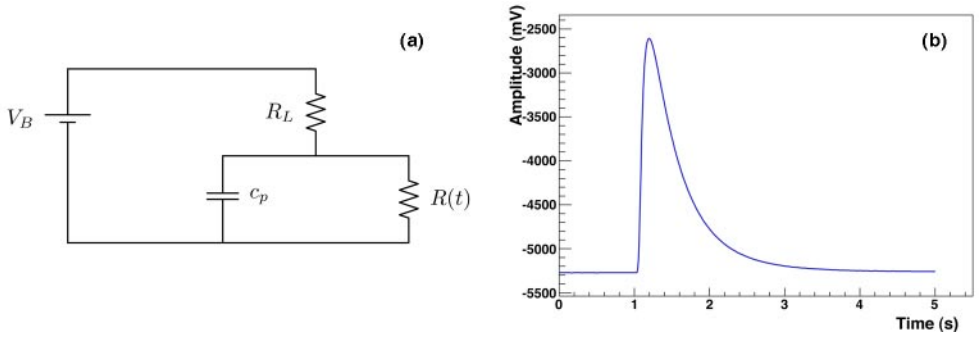


Fig. 2. – Biasing circuit of the thermistor (a) and a typical signal read through it (b).

the circuit components are: $V_{\mathrm{B}} \approx 5\,\mathrm{V}$, $R_{\mathrm{L}} \approx 50\,\mathrm{G\Omega}$, $c_{\mathrm{p}} \approx 400\,\mathrm{pF}$. The signal $V(t)$ is then amplified (gain $= 5000\,\mathrm{V/V}$), filtered by a six-poles anti-aliasing Bessel filter (frequency bandwith $\nu_{\mathrm{B}} = 12\,\mathrm{Hz}$) and sampled by an analog-to-digital converter (sampling frequency $\nu_{\mathrm{ADC}} = 125\,\mathrm{Hz}$, duration of the acquisition window $\Delta t = 5.008\,\mathrm{s}$).

An example of an acquired signal is shown in fig. 2(b). Its amplitude gives information about the quantity of energy released in the bolometer, whereas the baseline depends on the temperature of the detector before the interaction.

## 3. – Non-linearities of the response function

The main features of the recorded signal are the amplitude and the shape. The shape parameters used in this study are the rise time and the decay time, defined as the time difference between the 10% and the 90% of the pulse height and between the 90% and 30%, respectively. The analysed data come from calibration measurements realized facing a $^{232}$Th external source to a set of 26 crystals. Some crystals were equipped with one thermistor and others with two, so that the total number of channels to be analysed is 36. Hereafter channels are labeled as in the electronics setup, that ranges from 1 to 72. The resulting energy spectrum has a range from few keV up to about 3 MeV. In this configuration the amplitude of the pulses is about 0.1 mV/MeV $\times$ gain, the rise time and the decay time are of order 80 ms and 500 ms, respectively. The conversion from signal amplitude to energy is complicated, but feasible through the calibration procedure.

Nevertheless the signal exhibits other non-linearities:

1. Rise time and decay time depend on the energy of the pulse and are anticorrelated and correlated with the energy, respectively (see fig. 3(a) and fig. 3(b)). This effect makes the pulse shape discrimination in the data analysis difficult.
2. The amplitude of a pulse with fixed energy relies on the baseline (see fig. 4) and then on the working bolometer temperature. This leads to a worsening of the energy resolution.

Previous studies [11] have traced back these non-linearities predominantly to the thermistor behaviour and to the biasing circuit one. Consequently, we can neglect the further effects of the entire thermal circuit constituted by the bolometer, the thermistor and the supports, whose capacitances and conductivities are potentially dependent on the temperature and in general hard to measure with precision and independently one from the other.

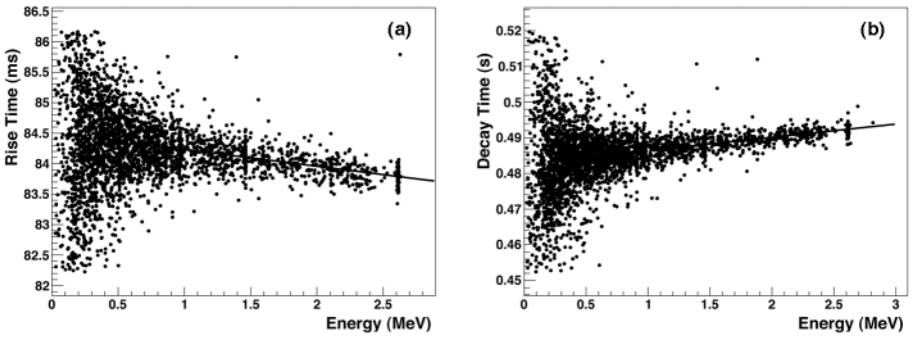


Fig. 3. – Pulse shape parameters *vs.* energy in channel 1: rise time (a) and decay time (b) are anticorrelated and correlated with energy, respectively.

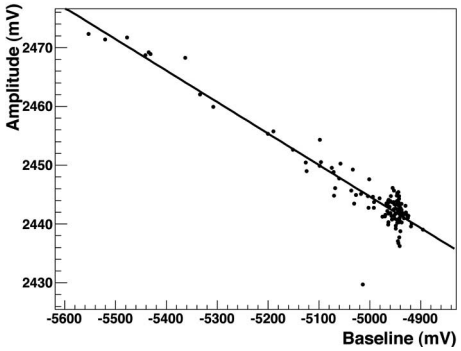


Fig. 4. – Slope amplitude *vs.* baseline for 2615 keV $\gamma$'s of $^{208}$Tl (from the $^{232}$Th decay chain), channel 35.

In particular, the thermistor behaviour explains the trend of the decay time and the dependence of the amplitude of the pulse with the baseline, whereas the rise time trend is ascribed to the biasing circuit.

## 4. – Thermal response analysis: a first algorithm

In order to linearize the data, an algorithm has been already developed [11]. To derive the algorithm, first of all we have to separate two contribution in $R(t)$ and $V(t)$: the former, due to the baseline temperature $T$, and the latter, due to the signal

$$R(t) = R(T) + \Delta R(t), \qquad V(t) = V(T) + \Delta V(t). \tag{2}$$

Solving the biasing circuit in fig. 2(a), we obtain the differential equation relating resistance and voltage variations:

$$\left[\frac{R_{\mathrm{L}} + R(T) + \Delta R(t)}{R(T) + \Delta R(t)}\right]\left[V_{\mathrm{B}}\frac{R(T)}{R(T) + R_{\mathrm{L}}} + \Delta V(t)\right] - V_{\mathrm{B}} + R_{\mathrm{L}} c_{\mathrm{p}} \Delta V'(t) = 0. \tag{3}$$

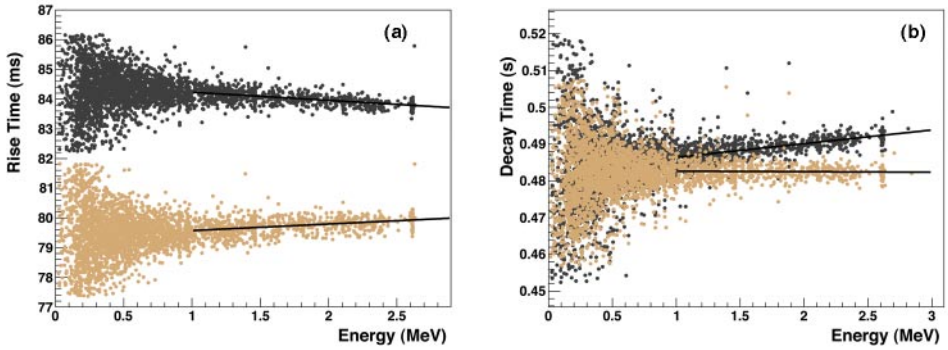


Fig. 5. – Pulse shape parameters *vs.* energy in channel 1: rise time (a) and decay time (b), in STD (dark gray) and TR (light gray) analysis.

From the previous equation we can extract $\Delta R(t)$ from $\Delta V(t)$ and other measurable quantities:

$$\Delta R(t) = -\frac{\Delta V(t)[R(T)+R_{\mathrm{L}}] + R_{\mathrm{L}}R(T)c_{\mathrm{p}}\Delta V'(t)}{\Delta V(t) + R_{\mathrm{L}}c_{\mathrm{p}}\Delta V'(t) + V_{\mathrm{B}}R_{\mathrm{L}}/[R(T)+R_{\mathrm{L}}]}\,. \tag{4}$$

Considering that the resistance variation $\Delta R(t)$ in terms of the temperature variation $\Delta T(t)$ can be approximated as

$$\Delta R(t) \simeq R(T)\left[\exp\left[-\frac{\eta\Delta T(t)}{T}\right]-1\right], \tag{5}$$

where $\eta$ is the thermistor sensitivity, defined as $\eta = |\mathrm{d}\log R|/|\mathrm{d}\log T| \approx 10$, we can obtain the thermal response of the detector, that is a quantity proportional to the temperature variation:

$$\Delta S = \frac{\eta}{T}\Delta T(t) = -\log\left[1+\frac{\Delta R(t)}{R(T)}\right]. \tag{6}$$

This algorithm converts the acquired samples $\Delta V(t)$ in signals proportional to the temperature variation $\Delta T(t)$ on the thermistor. It has also the advantage to be reliant only on parameters easily measurable, while the unknown quantities are hidden in the scale factor $\eta/T$, which is ininfluent in the perspective of removing the non-linearities.

The application of the thermal response algorithm on the data gives the results represented in figs. 5, 6 and 7. The thermal response (TR) data, labeled by light gray points, are compared with the data already shown in fig. 3 and fig. 4, labeled by dark-gray points, that can be defined as the standard (STD) data. The shape of the TR pulses is less dependent on the energy, especially in the case of the decay time, and also the dependence of the amplitude from the baseline has been reduced. We also notice that the rise time of the TR data is lower than the STD data, because the low pass filter of the biasing circuit has been deconvoluted (fig. 5(a)).

Nevertheless, there are some residual non-linearities in the response function. Almost all the analysed channels have an amplitude slope of the 2615 keV $\gamma$'s of $^{208}$Tl which is

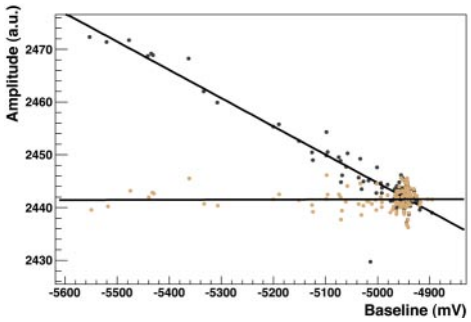


Fig. 6. – Slope amplitude *vs.* baseline for 2615 keV $\gamma$'s of $^{208}$Tl in STD (dark gray) and TR (light gray) analysis, channel 35.

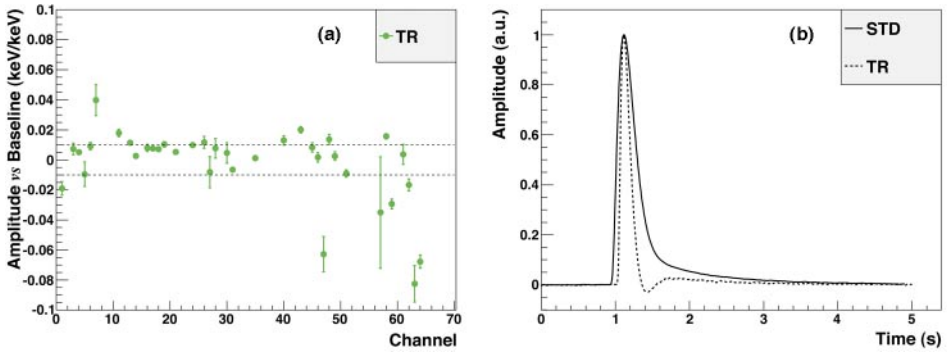


Fig. 7. – Residual non-linearities: amplitude slope for all channels according to TR analysis (a) and the pulse shape of channel 47 for STD and TR analysis (b).

contained in a $\pm 0.01$ keV/keV range, but there are some outliers, like the channels 47, 57, 63 and 64 (fig. 7(a)). The same channels have also a particular shape of the TR signal. After reaching its maximum, the TR pulse goes down and then up again (see fig. 7(b)). This behaviour is ascribed to the electrothermal feedback phenomenon. According to this, the biasing current produces a power dissipation which warms up the thermistor and reduces its resistance; when the temperature increases, the variation of the power dissipated on the thermistor is negative and decreases the signal. In the STD pulse this effect is masked by the low-pass filter originated from the the thermistor resistance and the parasitic capacitances.

## 5. – Insertion of a RC-filter with constant cutoff

A first improvement of the algorithm proposed in the previous section can be achieved applying a low-pass filter with constant cutoff to the TR data. In this way we try to get a shape of the transformed pulse more similar to the original one, mantaining at the same time the non-linearities removal.

If we solve the biasing circuit approximately, using $R_L \gg R$ and $R_L \gg \Delta R(t)$, we obtain the equation

$$\Delta V(t) + [R(T) + \Delta R(t)] c_{\mathrm{p}} \Delta V'(t) = -\frac{V_B}{R_L} \Delta R(t). \tag{7}$$

This expression has the form of a low-pass filter, with a cutoff that depends on the input signal $\Delta R(t)$: the higher is its absolute value, the higher is the cutoff, making the pulse faster. Since $R(T)c_{\mathrm{p}} \sim 30\,\mathrm{ms}$, this effect is prevailing on the rise time, while on the decay time there is a possible competition with the opposite effect determined by the thermistor, as mentioned in sect. **3**. Considering eq. (7), if we delete the dependence of the cutoff on $\Delta R$, which is the non-linearity source, we obtain the expression of a RC-filter with constant cutoff

$$\Delta V(t) + R(T) c_{\mathrm{p}} \Delta V'(t) = -\frac{V_{\mathrm{B}}}{R_{\mathrm{L}}} \Delta R(t), \tag{8}$$

whose more general form is

$$V_{\mathrm{out}}(t) + R c_{\mathrm{p}} \frac{\mathrm{d}V_{\mathrm{out}}(t)}{\mathrm{d}t} = V_{\mathrm{in}}(t). \tag{9}$$

This equation can be easily discretized. Assuming that the samples of the input and output are taken at evenly spaced points in time separated by $\Delta t$, let the samples of $V_{\mathrm{in}}$ be represented by the sequence $(x_1, x_2, \ldots, x_{\mathrm{n}})$ and let the samples of $V_{\mathrm{out}}$ be represented by the sequence $(y_1, y_2, \ldots, y_{\mathrm{n}})$, which corresponds to the same points in time. After these substitutions and the rearrangement of the terms, we can obtain the recurrence relation

$$y_{\mathrm{i}} = x_{\mathrm{i}} \left( \frac{\Delta t}{RC + \Delta t} \right) + y_{\mathrm{i}-1} \left( \frac{RC}{RC + \Delta t} \right), \tag{10}$$

where the former addend represents the input contribution, while the latter constitutes the inertia from the previous output: as the time constant RC increases, the output samples $(y_1, y_2, \ldots, y_{\mathrm{n}})$ respond more slowly to a change in the input samples $(x_1, x_2, \ldots, x_{\mathrm{n}})$.

The results from the application of the new algorithm (10) implemented as a filter on TR data are represented in fig. 8. The pulse resulting from this analysis, called "TR+RC", does not exhibit the TR trend and it reproduces the original pulse shape (fig. 8(b)). In addition, the residual slope has been reduced (fig. 8(a)). Notice that it is the amplitude which was modified, while the baseline is unchanged.

## 6. – The electrothermal feedback

In order to develop a more complete model of the bolometer response function, we need to make explicit the contribution due to the electrothermal feedback to which we attribute the shape of the TR signal. The feedback phenomenon is a potential source of non-linearities, so it has to be investigated and possibly removed.

In the electrothermal models cited in sect. **1**, a temperature variation $\Delta T$ into a bolometer, that has a heat capacitance $C$ and is connected with a thermal bath through

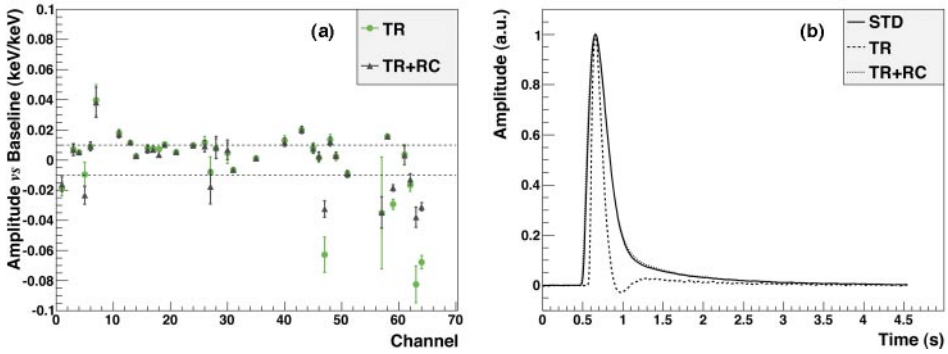


Fig. 8. – Analysis with RC inserted: amplitude slope for all channels according to TR and TR+RC analysis (a) and the pulse shape of channel 47 for STD, TR and TR+RC analysis (b).

a conductance $K$, is traced back to an external incident power (the signal) $W$ and to the power dissipated into the detector by the thermistor $\Delta P$, according to the equation

$$C\Delta T'(t) + K\Delta T(t) = W(t) + \Delta P(t). \tag{11}$$

In our analysis we have that $\Delta T = (T/\eta)\Delta S$, therefore the power attributed to the signal can be expressed as

$$W(t) = \frac{CT}{\eta}\Delta S'(t) + \frac{KT}{\eta}\Delta S(t) - \Delta P(t). \tag{12}$$

Rescaling this equation by the factor $KT/\eta$, we obtain the further formula for the thermal response $W^*$

$$W^*(t) = \Delta S(t) + \frac{C}{K}\left(\Delta S'(t) - \frac{\eta}{TC}\Delta P(t)\right), \tag{13}$$

where the former term is the thermal response derived in sect. **4** and the latter represents the additional share due to the feedback.

The $\Delta S'$ quantity can be immediately calculated from $\Delta S$, while $\Delta P$ can be calculated as follows. Defining $\Delta P(t) = P(t) - P(T)$, we have that the power dissipated in static conditions is

$$P(T) = \left(\frac{V_{\mathrm{B}}}{R_{\mathrm{L}} + R(T)}\right)^2 R(T), \tag{14}$$

while in dynamic conditions the power can be calculated from the biasing circuit expression (3) and it assumes the form

$$P(t) = \frac{V(t)^2}{R(t)} = P(T)\left\{\frac{\left[1 + \frac{\Delta V(t)}{V_{\mathrm{B}}}\left(1 + \frac{R_{\mathrm{L}}}{R(T)}\right)\right]^2}{1 + \frac{\Delta R(t)}{R(T)}}\right\}. \tag{15}$$

Therefore in eq. (13) also $\Delta P(t)$ is a computable quantity. Nevertheless, in the same equation the two parameters $C/K$ and $C/K * \eta/(TC) = \eta/(TK)$ include the quantities $C$, $K$, $T$ that are not known with precision. In eq. (11) $C$ and $K$ are referred generically to the bolometer, whereas we have the entire thermal circuit composed by the bolometer, the thermistor and the supports, whose capacitances and conductances cannot be measured independently.

We are working to develop procedures to estimated the two parameters $C/K$ and $\eta/(TK)$ *a posteriori* from the data, in such a way that the detector response is optimized, that is, the non-linearities are reduced. From CUORICINO measurements [5], preliminary reckonings are $C/K \sim 0.1\,\mathrm{s}$, $\eta/(TK) \sim 10^{13}\,\mathrm{W}^{-1}$. Since the order of magnitude of the $C/K$ value is comparable to the rise time one, we can expect a correction to the trend of this shape parameter.

Finally, the effects of the thermal response algorithms on the calibration function will be studied. The calibration function is usually parametrized with a third-order polynomial function in the standard analysis of $TeO_2$ detectors. To parametrize the function, the detector is exposed to the calibration source so that the entire range of energies is populated. In CUORE the calibration procedure could take long time (up to one week per month), reducing the live time of the experiment. If the calibration function were reduced to a line, the calibration procedures of CUORE could be substantially shortened, thus increasing the sensitivity of the experiment to $0\nu$DBD.

* * *

I am very grateful to the members of the CUORE-Roma Collaboration. I wish to thank in particular F. Ferroni and M. Vignati for their support and for the supervision of this work.

REFERENCES

[1] Ardito R. *et al.*, arXiv:hep-ex/0501010, unpublished.
[2] Wang N., Wellstood F. C., Sadoulet B., Haller E. E. and Beeman J., *Phys. Rev. B*, **41** (1990) 3761.
[3] Itoh K. M., Haller E. E., Hansen W. L., Beeman J. W., Farmer J. W., Rudnev A., Tikhomirov A. and Ozhogin V. I., *Appl. Phys. Lett.*, **64** (1994) 2121.
[4] Jones R. C., *J. Opt. Soc. Am.*, **43** (1953) 1.
[5] Alessandrello A., Brofferio C., Camin D., Cremonesi O., Giuliani A., Pavan M., Pessina G. and Previtali E., *IEEE Trans. Nucl. Sci*, **40** (1993) 649.
[6] McCammon D., *Proceedings of the 10th International Workshop on Low Temperature Detectors, Genoa, 2003*, *Nucl. Instrum. Methods Phys. Res. A*, **520** (2004) 11.
[7] Barucci M., Brofferio C., Giuliani A., Gottardi E., Peroni I and Ventura G., *J. Low Temp. Phys.*, **123** (2001) 303.
[8] Mott N. F., *Philos. Mag.*, **19** (1969) 835.
[9] Efros A. and Shklovskii B., *Electronic Properties of Doped Semiconductors* (Springer-Verlag, Berlin) 1984.
[10] Itoh K. M., Haller E. E., Beeman J. W., Hansen W. L., Emes J., Reichertz L. A., Kreysa E., Shutt T., Cummings A., Stockwell W., Sadoulet B., Muto J., Farmer J. W. and Ozhogin V. I., *Phys. Rev. Lett.*, **77** (1996) 4058.
[11] Vignati M., *J. Appl. Phys.*, **108** (2010) 084903.